

ON THE DYNAMIC RIDE FORCES OF THE VEHICLE-TRACK SYSTEM

Mădălina DUMITRIU

University Politehnica of Bucharest
Splaiul Independenței nr. 313, 77206 București, Romania
madalinadumitriu@yahoo.com

Abstract

This paper presents the dynamic ride forces generated at the wheel-rail interface during the running of a railway vehicle over a track with vertical irregularities derived from the overlying of the local discontinuities coming from the track joints and geometric irregularities. The dynamic ride forces are obtained from numerical simulations, developed on the basis of a ‘rigid body’ type vehicle with 10 degrees of freedom, where the inputs are represented by the track irregularities, analytically introduced. The results here featured make a point from the influence of velocity and the amplitude of the track geometric irregularities upon the value of the dynamic ride forces, depending on the axle position within the running gear.

Key words: railway vehicle, track irregularities, joint, dynamic ride forces, geometric filtering effect

1. Introduction

Dynamic contact forces occur and overlie upon the static forces at the wheel-rail interface during the running of the railway vehicles over the track geometric irregularities, the discontinuities of the rails (joints, switches, crossings), the irregularities of the rolling surfaces of the tracks [1, 2], or when one of the vehicle wheel is running over a local defect of its own rolling surface (eg. the flat point) [3]. In dependence on their size, the dynamic ride forces can trigger important stresses of the vehicle and track structures, which will have an impact upon both the wheel mechanical resistance, the other components of the running gear and the rail mechanical resistance [4 - 6]. Also, the wear of the wheel-rail rolling surfaces [7] should be mentioned, along with the presence of the rolling noise [8, 9].

Under such conditions, the limitation of the dynamic ride forces is fully required, as it is one of the homologation criteria for the railway vehicles in terms of the dynamic behavior for the fatigue resistance of the track [10, 11]. The limitation of the dynamic ride forces to a level where to provide the best performance of the vehicle needs to be considered even since the designing stage, which implies the study of the influence of the vehicle parameters upon its dynamic response [12, 13].

The paper examines the vertical dynamic forces that occur at frequencies lower than cca. 20 Hz - the dynamic ride forces. They come from the dynamic response of the suspended masses of the vehicle

during the travelling over the track irregularities. On the other hand, the dynamic forces of over 20 Hz derive from the wheel-rail structural vibrations [4, 14, 15]. In fact, the track vertical irregularities represented by the local discontinuities of the rail in the joints are taken into account, since they are considered to be the most critical that the wheel is bound to cross, over which the track geometric irregularities are overlapping along the rail segments.

The dynamic ride forces are determined by means of certain applications of numerical simulation, while considering various speed conditions of a four-wheel vehicle. They are developed based on a mechanical model of the ‘rigid body’ type vehicle, with 10 degrees of freedom corresponding to the carbody bounce and pitch motions and also of the bogies and the vertical displacement of the axles. It is thereby pointed out that the dynamic ride forces do not have a consistent increase along the velocity, thus explained by the geometric filtering effect from the vehicle wheelbases [16, 17].

2. The analytical representation of the track irregularities on the tracks with joints

The vertical motions of the axles depend on the profile of the track irregularities being crossed and on the vehicle speed. These motions are further conveyed to the suspended masses of the vehicle, thus generating and maintaining their vibrations.

As a principle, the analytical representation of the

motions of wheelsets has to be as simple as possible and also to easily lead to a theoretical evaluation of the motions in the suspended masses, as close to reality as available.

If the perturbation function is known, expressing the time-dependent motion of the axle, the dynamic forces generated at the wheel-rail interface can be theoretically evaluated and also be established to what extent the dynamic performance of the vehicle can be improved by changing the main parameters of construction. To this purpose, the recorded profile of the track which is obtained with railway vehicles specially equipped to measure the track imperfections can be used. Very often, such information is not available and, in this case, an analytical description of the track irregularities can be utilized.

A quite close to reality evaluation of the shocks transmitted to the vehicle is done on the tracks with joints, substituting the registered profile of the joint with a profile (fig. 1) as shown in the relation [18]

$$\eta_j = \frac{H_0}{2} \left(1 - \cos \frac{2\pi x}{L_0} \right) \quad (1)$$

for $0 \leq x \leq L_0$, where H_0 is the amplitude of the track irregularity given by the joint and L_0 – the length of the track irregularity in the joint. The length of the irregularity coming from the joint varies between 1 and 5 meters, in an average of $L_0 = 2.5$ m, where the medium amplitude is $H_0 = 1$ cm.

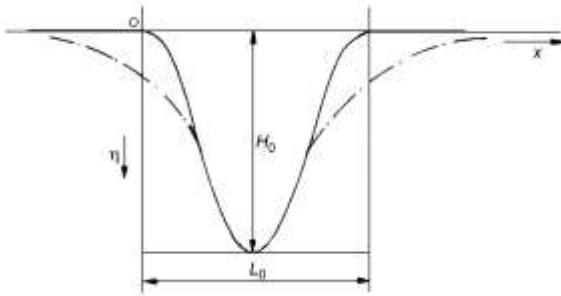


Fig. 1: The analytical representation of the joint profile: - · - ·, the curve of the joint registered profile; —, the curve of the joint profile, according to the equation (1)

The tracks with joints can also feature vertical irregularities of a geometric nature that mainly come from the imperfections in construction, the track exploitation, the change in the track infrastructure, as a response to the action of the environment factors or the soil motions [19]. The vehicle motion will be here as a resultant from the overlapping of the joint motion over the one coming from the wheels crossing the geometric irregularities in the track, existent along the rail segments.

While considering that the track geometric irregularities are in a proximately sinusoidal form of amplitude H_1 , and L represents the length of the rail segment, the equation for the profile of such irregularities can have a simplified form

$$\eta_t = H_1 \cos \frac{4\pi x}{L}, \quad (2)$$

where $x = Vt$, with V is the vehicle speed. The values of H_1 , generally varies between $H_1 = 0.25H_0$ and $H_1 = 0.5H_0$, with an average of $H_1 = 0.35H_0$.

In this case, the equation corresponding to the axle motion is

$$\eta_w = \eta_t = H_1 \cos 2\omega t. \quad (3)$$

where $2\omega = 4\pi V/L$ is the pulsation of the axle vertical vibrations.

Under the effect of the axle perturbation motion, the vehicle forced vibrations will be also harmonic, with the same pulsation 2ω . When overlying the vibrations derived from the joints, which are aperiodic, the resulting motion will be also aperiodic. The experience has proved that this overlapping mode of the two types of vibrations is achieved only if the natural damped vibrations of the vehicle coming from the joints have enough time to completely dampen themselves prior to the occurrence of a new shock from the next joint. If not, it is considered that the joints constitute a periodic disturbance in their succession, which also triggers periodic vibrations, of a pulsation equal with the pulsation coming from the succession of the joints, namely $\omega = 2\pi v/L$ [18].

For this situation, the track registered profile can be roughly substituted with a curve (fig. 2), with the equation

$$\eta = \frac{H_0}{2} \left(1 - \cos \frac{2\pi x}{L} \right) + H_1 \cos \frac{4\pi x}{L}, \quad (4)$$

and the axles will generate a disturbance as in the function below

$$\eta_w = \eta = \frac{H_0}{2} (1 - \cos \omega t) + H_1 \cos 2\omega t. \quad (5)$$

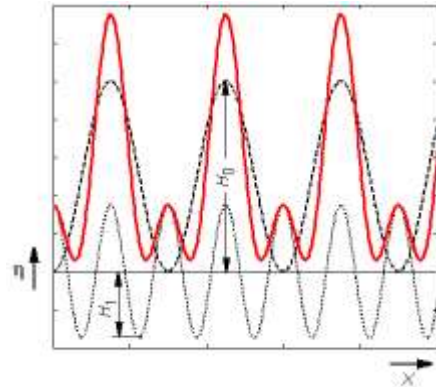


Fig. 2: The representation of the track irregularities on the tracks with joints: —, η ; - - -, η_j ; ·····, η_t ;

The fig. 2 features the curve that replaces the track registered profile from the equation (4), as well as the curves corresponding to the joint profile (η_j), and the

profile of the track geometric irregularities, respectively (η_i)

$$\eta_j = \frac{H_0}{2} \left(1 - \cos \frac{2\pi x}{L} \right); \quad \eta_i = H_1 \cos \frac{4\pi x}{L}. \quad (6)$$

3. The mechanical model and the equation of motion for the vehicle

The figure 3 shows the mechanical model of a four-axle, two-stage suspension vehicle. It travels at a constant speed V along a perfectly rigid track that presents vertical irregularities coming from the overlapping of the local irregularities from the joints and of the irregularities of a geometric nature already present along the rail segments, analytically described in the equation (4). Against each wheelset, such irregularities will be in the below form, for $i = 1 \dots 4$,

$$\eta_i = \frac{H_0}{2} \left(1 - \cos \frac{2\pi x_i}{L} \right) + H_1 \cos \frac{4\pi x_i}{L}, \quad (7)$$

where x_i is given by the position of the wheelset in the vehicle, namely

$$\begin{aligned} x_1 &= x; & x_2 &= x - a_b; \\ x_3 &= x - 2a_c; & x_4 &= x - 2a_b - 2a_c. \end{aligned}$$

The model of the vehicle comprises seven rigid bodies that represent the vehicle carbody, the suspended masses of the two bogies and four wheelsets. They are connected among themselves via Kelvin-Voigt systems, that model the suspension stages.

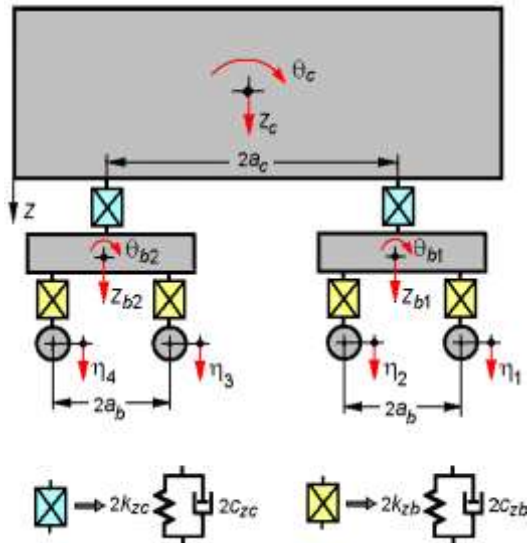


Fig. 3: The mechanical model of the vehicle.

The perturbation motions of the wheelsets generate forced bounce (z_c) and pitch vibrations (θ_c) of the carbody and forced bounce ($z_{b1,2}$) and pitch ($\theta_{b1,2}$) vibrations of the bogies.

The equations of the bounce and pitch carbody motions are as follows:

$$\begin{aligned} m_c \ddot{z}_c + 2c_{zc} [2\dot{z}_c - (\dot{z}_{b1} + \dot{z}_{b2})] + \\ + 2k_{zc} [2z_c - (z_{b1} + z_{b2})] = 0; \end{aligned} \quad (8)$$

$$\begin{aligned} J_c \ddot{\theta}_c + 2a_c c_{zc} [2a_c \dot{\theta}_c - (\dot{z}_{b1} - \dot{z}_{b2})] + \\ + 2a_c k_{zc} [2a_c \theta_c - (z_{b1} - z_{b2})] = 0, \end{aligned} \quad (9)$$

where $2a_c$ is the carbody wheelbase, m_c is carbody mass and J_c - the inertia moment.

The equation of the bounce motion for the front bogie is

$$\begin{aligned} m_b \ddot{z}_{b1} + 2c_{zc} (\dot{z}_{b1} - \dot{z}_c - a_c \dot{\theta}_c) + \\ + 2k_{zc} (z_{b1} - z_c - a_c \theta_c) + \\ + 2c_{zb} [2\dot{z}_{b1} - (\dot{\eta}_1 + \dot{\eta}_2)] + \\ + 2k_{zb} [2z_{b1} - (\eta_1 + \eta_2)] = 0 \end{aligned} \quad (10)$$

and for the rear one writes as

$$\begin{aligned} m_b \ddot{z}_{b2} + 2c_{zc} (\dot{z}_{b2} - \dot{z}_c + a_c \dot{\theta}_c) + \\ + 2k_{zc} (z_{b2} - z_c + a_c \theta_c) + \\ + 2c_{zb} [2\dot{z}_{b2} - (\dot{\eta}_3 + \dot{\eta}_4)] + \\ + 2k_{zb} [2z_{b2} - (\eta_3 + \eta_4)] = 0, \end{aligned} \quad (11)$$

where m_b is the bogie mass.

Similarly, the equations of the pitch motion for the two bogies are:

- for the front bogie

$$\begin{aligned} J_b \ddot{\theta}_{b1} + 2a_b c_{zb} [2a_b \dot{\theta}_{b1} - (\dot{\eta}_1 - \dot{\eta}_2)] + \\ + 2a_b k_{zb} [2a_b \theta_{b1} - (\eta_1 - \eta_2)] = 0; \end{aligned} \quad (12)$$

- for the rear bogie

$$\begin{aligned} J_b \ddot{\theta}_{b2} + 2a_b c_{zb} [2a_b \dot{\theta}_{b2} - (\dot{\eta}_3 - \dot{\eta}_4)] + \\ + 2a_b k_{zb} [2a_b \theta_{b2} - (\eta_3 - \eta_4)] = 0, \end{aligned} \quad (13)$$

where $2a_b$ represents the bogie wheelbase and J_b is the inertia moment.

To calculate the dynamic ride forces on wheels, the starting point is the equations of motion for each wheelset, written as such:

- for the wheelsets of the front bogie

$$\begin{aligned} m_o \ddot{\eta}_{1,2} + 2c_{zb} (\dot{\eta}_{1,2} - \dot{z}_{b1} \mp a_b \dot{\theta}_{b1}) + \\ + 2k_{zb} (\eta_{1,2} - z_{b1} \mp a_b \theta_{b1}) - 2\Delta Q_{1,2} = 0. \end{aligned} \quad (14)$$

- for the wheelsets of the rear bogie

$$\begin{aligned} m_o \ddot{\eta}_{3,4} + 2c_{zb} (\dot{\eta}_{3,4} - \dot{z}_{b2} \mp a_b \dot{\theta}_{b2}) + \\ + 2k_{zb} (\eta_{3,4} - z_{b2} \mp a_b \theta_{b2}) - 2\Delta Q_{3,4} = 0. \end{aligned} \quad (15)$$

where m_o is the wheelset mass, and ΔQ_i ($i=1$ to 4) are the dynamic ride forces; these forces corresponding to the wheels of an wheelset have the same value.

4. Numerical application

This section points out at the results coming from the numerical simulations regarding the extent of the dynamic ride forces derived from the model in the previous section.

The parameters of the numerical model of the vehicle are included in table 1, and they are representative for a passenger car. Similarly, the length of the rail segment is $L = 15$ m, and the following reference values $H_0 = 0.01$ m; $H_1 = 0.35H_0$ are considered as the geometric parameters of the track vertical irregularities:

Table 1: The parameters of the numerical model of the vehicle

$m_c = 34000$ kg	$2k_{zc} = 1.2$ MN/m
$m_b = 3200$ kg	$2c_{zc} = 34.44$ kNs/m
$m_o = 1650$ kg	$4k_{zb} = 4.4$ MN/m
$J_c = 1963840$ kgm ²	$4c_{zb} = 52.21$ kNs/m
$J_b = 2048$ kgm ²	$2a_c = 19$ m; $2a_b = 2.56$ m

The fig. 4 illustrates the dynamic ride forces, calculated at the speeds of 40 km/h, 80 km/h and 120 km/h. It should be firstly noted that the dynamic ride forces corresponding to the axles of each bogie are in phase at 40 km/h but a phase difference occurs when the velocity increases. These differences become higher along with the speed. The diagrams in the fig. 4 also feature the rise of the dynamic ride forces along with the speed. This aspect is further examined in the figure 5, which shows the maximum values of these forces, calculated at various speeds ranging from 40 km/h to 140 km/h.

What can be noticed is that the dynamic ride forces generally increase along with the speed, irrespective of the wheelset position in the vehicle, but the rise is not constant. The most relevant examples can be given for the wheelsets of the rear bogie. Thus, for axle 3, the dynamic ride forces constantly increase with the speed, reaching 5194 N for $V = 80$ km/h. Further, for the speed of 100 km/h, ΔQ_3 lowers to 2006 N, then goes up again to 2650 N for $V = 120$ km/h. Likewise, for axle 4, the dynamic ride forces show a constant increase within the interval of 40 ... 80 km/h, with the value of 7117 N at 80 km/h. Should the speed rises to 100 km/h, ΔQ_4 decreases to 5000 N. At the speed of 120 km/h, the dynamic ride forces increase to 5530 N and ΔQ_4 has the value of 6977 N for 140 km/h.

The issues above can be explained via the geometric filtering effect coming from the wheelbases of the vehicle. The geometric filtering effect is an essential feature of the behaviour of vertical vibrations in the railway vehicles, mainly due to the manner in which the excitations coming from

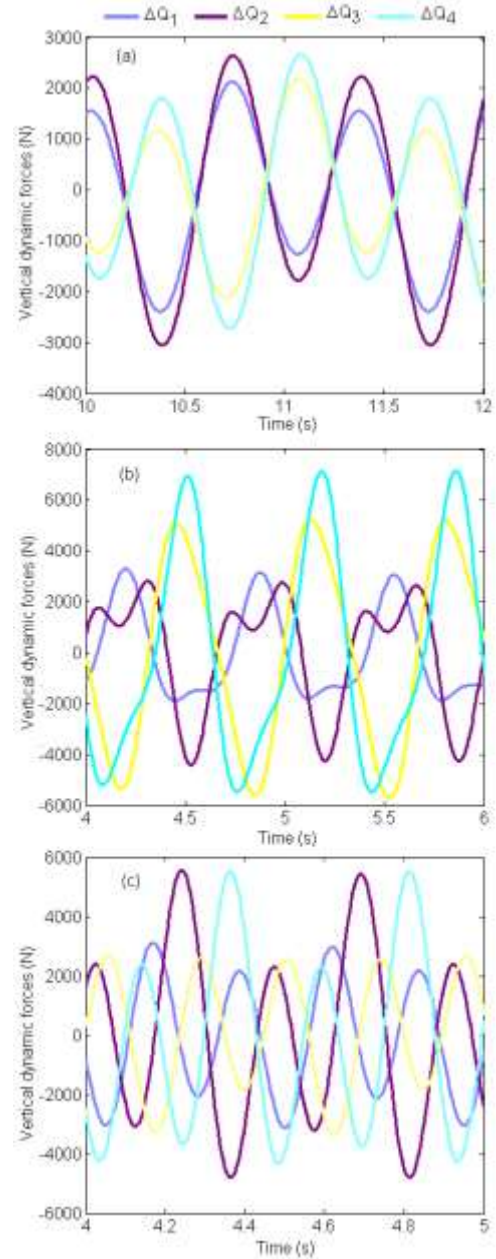


Fig. 4: Dynamic ride forces:
(a) $V = 40$ km/h; (b) 80 km/h; (c) 120 km/h.

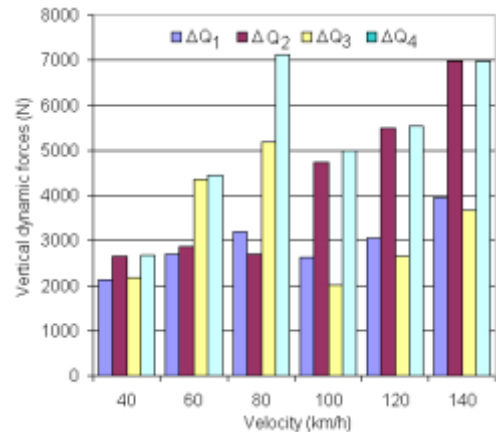


Fig. 5: The velocity influence upon the value of the dynamic ride forces.

the track are conveyed to the suspended masses via the wheelsets, irrespective of the suspension characteristics. Practically speaking, the geometric filtering effect is the result of the displacement between the vertical movements in the wheelsets coming from moving on a track with irregularities, a displacement that derives from the wheelset position in the assembly of the running gear and the vehicle velocity. This fact gives the geometric filtering a selective nature, depending on the vehicle wheelbases and on velocity and, to that end, a differentiated efficiency along the vehicle on the one hand and velocity regime, on the other hand [16, 17].

A last remark is the fact that the highest values of the dynamic ride forces are recorded at the rear wheelsets of each bogie. There are, however, two exceptions, corresponding to the velocities of 40 km/h and 80 km/h where the dynamic ride forces have high values in both wheelsets of the rear bogie.

Table 2: The increase of the dynamic ride forces.

Velocity [km/h]	ΔQ_1	ΔQ_2	ΔQ_3	ΔQ_4
40	79.41 %	87.13%	68.36 %	77.26 %
80	20.91 %	37.57 %	4 %	16.92 %
120	80.41 %	63.42 %	95.4 %	63.24 %

Figure 6 features the increase of the dynamic ride forces along with the rise in the amplitude of the track geometric irregularities. It is evident that this increase can be significant, depending on velocity and the wheelset position in the vehicle. This is shown in table 2, which includes the percentage growth of the dynamic ride forces in the four axles of the vehicle when doubling H_1 (from $0.25H_0$ to $0.5H_0$).

5. Conclusions

The response of the vehicle during crossing over the track vertical irregularities will generate dynamic ride forces, whose frequency spectrum ranges up to circa 20 Hz. The value of such forces depends on the vehicle velocity and on the characteristics of the track irregularities, herein discussed. For this purpose, the dynamic ride forces have been calculated for a four-axle vehicle during running over a track with joints.

A series of relevant observations relies on the results thus derived. It has therefore shown that the dynamic ride forces corresponding to the axles of the same bogie are in phase for low velocities; there will be phase differences when the speed increases – the higher the velocity, the higher the difference. Another essential issue regards the fact that the dynamic ride forces do not have a constant increase along with the velocity, explained by the geometric filtering effect given by the distances between the vehicle axles. Ultimately, the dynamic ride forces can have a significant rise in dependence on the velocity, during the increase in the amplitude of the track irregularities.

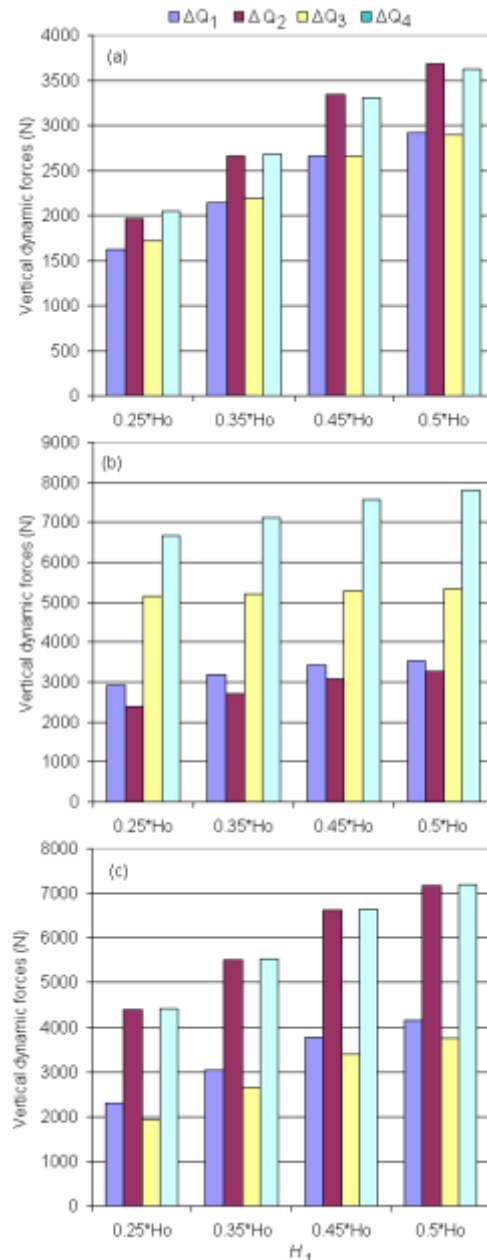


Fig. 6: The influence of the amplitude of the track geometric irregularities upon the value of the dynamic ride forces: (a) $V = 40$ km/h; (b) 80 km/h; (c) 120 km/h.

References

- [1] Wu T.X., Thompson D.J. (2001), *Vibration analysis of railway track with multiple wheels on the rail*, Journal of Sound and Vibration, vol. 239, pp. 69-97.
- [2] Steenbergen, M. (2006), *Modelling of wheels and rail discontinuities in dynamic wheel-rail contact analysis*, Vehicle System Dynamics, vol. 44, no. 10, pp. 763-787.
- [3] Wu T. X., Thompson D.J. (2002), *A hybrid model for the noise generation due to railway wheel flats*, Journal of Sound and Vibration, vol. 251, pp. 115-139.

- [4] Mazilu, T. (2008), *Vibrații roată-șină* (Wheel rail vibrations), Ed. MatrixRom, București.
- [5] Gullers, P., Andersson, L., Lundén, R. (2008), *High-frequency vertical wheel-rail contact forces—Field measurements and influence of track irregularities*, *Wear*, vol. 265, Iss. 9–10, pp. 1472–1478.
- [6] Karttunen, K., Kabo, E., Ekberg, A. (2014), *The influence of track geometry irregularities on rolling contact fatigue*, *Wear*, vol. 314, iss. 1–2, pp. 78–86.
- [7] Oostermeijer, K.H. (2008), *Review on short pitch rail corrugation studies*, *Wear*, vol. 265, pp. 1231-1237.
- [8] Mazilu, T. (2003), *Confortul la materialul rulant* (Comfort at the rolling stock), Ed. MatrixRom, București.
- [9] Thompson, D.J. (1988), *Wheel/rail contact noise: development and detailed evaluation of a theoretical model for the generation of wheel and rail vibration due to surface roughness*, ORE DT 204 (C 163), Utrecht.
- [10] UIC 518 Leaflet - 4th edition (2009), *Testing and approval of railway vehicles from the point of view of their dynamic behaviour – Safety – Track fatigue – Running behaviour*.
- [11] EN 14363/2013, *Railway applications - Testing and Simulation for the acceptance of running characteristics of railway vehicles - Running behaviour and stationary tests*.
- [12] Dumitriu, M. (2013), *Influence of the primary suspension damping on the vertical dynamic forces at the passenger railway vehicles*, UPB Scientific Bulletin, Series D: Mechanical Engineering, iss. 1, vol. 75, pp. 25-40.
- [13] Dumitriu, M. (2012), *On the dynamic vertical wheel-rail forces at low frequencies*, *Mechanical Journal Fiability and Durability*, issue supplement no. 1, pp. 11-17.
- [14] Thompson, D. (2009), *Railway noise and Vibration: mechanisms, modelling and means of control*, Elsevier, London.
- [15] Lyon, D. (2002), *A review dynamic vertical track forces*, *Research programme*, Report no. IFLT/111257.
- [16] Dumitriu, M. (2012), *Geometric filtering effect of vertical vibrations of railway vehicles*, *Analele Universității “Eftimie Murgu” Reșița*, no. 1, pp. 48-61.
- [17] Dumitriu, M. (2014), *Considerations on the geometric filtering effect of the bounce and pitch movements in railway vehicles*, *Annals of Faculty Engineering Hunedoara – International Journal of Engineering*, Tome XII, Fascicule 3, pp. 155-164.
- [18] Sebeșan, I. (2011), *Dinamica vehiculelor feroviare* (Dynamic of the railway vehicles), Ed. Matrix Rom, București.
- [19] Pombo, J., Ambrósio, J. (2012), *An alternative method to include track irregularities in railway vehicle dynamic analyses*, *Nonlinear Dynamics*, vol. 68, iss. 1-2, pp. 161-176.